



# Whiteite-(CaMnFe), a new jahnsite-group mineral from the Hagendorf-Süd pegmatite, Oberpfalz, Bavaria

Rupert Hochleitner<sup>1</sup>, Christian Rewitzer<sup>2</sup>, Ian E. Grey<sup>3</sup>, William G. Mumme<sup>3</sup>, Colin M. MacRae<sup>3</sup>, Anthony R. Kampf<sup>4</sup>, Erich Keck<sup>5</sup>, Robert W. Gable<sup>6</sup>, and Alexander M. Glenn<sup>3</sup>

<sup>1</sup>Mineralogical State Collection (SNSB), Theresienstrasse 41, 80333 Munich, Germany

<sup>2</sup>Stadtplatz 17, 93437 Furth im Wald, Germany

<sup>3</sup>CSIRO Mineral Resources, Private Bag 10, Clayton South, Victoria 3169, Australia

<sup>4</sup>Mineral Sciences Department, Natural History Museum of Los Angeles County, 900 Exposition Boulevard, Los Angeles, CA 90007, USA

<sup>5</sup>Algunderweg 3, 92694 Etzenricht, Germany

<sup>6</sup>School of Chemistry, University of Melbourne, Parkville, Victoria 3010, Australia

**Correspondence:** Ian E. Grey (ian.grey@csiro.au)

Received: 3 November 2022 – Revised: 12 January 2023 – Accepted: 16 January 2023 – Published: 14 February 2023

**Abstract.** Whiteite-(CaMnFe),  $\text{CaMn}^{2+}\text{Fe}_2^+\text{Al}_2(\text{PO}_4)_4(\text{OH})_2 \cdot 8\text{H}_2\text{O}$ , is a new whiteite-subgroup member of the jahnsite group from the Hagendorf-Süd pegmatite, Oberpfalz, Bavaria, Germany. It was found in vugs in an altered feldspar area of a specimen composed predominantly of rockbridgeite, with hureaulite and relic triphylite. Other associated minerals in small vugs in the specimen were strengite and laueite. Whiteite-(CaMnFe) occurs as sprays and clusters of colourless to pale yellow, rod-like crystals, with diameters of typically 10 to 50  $\mu\text{m}$  and lengths up to  $\sim 500 \mu\text{m}$ . The crystals are flattened on {001} and elongated along [010]. The measured density is  $2.80(2) \text{ g cm}^{-3}$ . Optically, whiteite-(CaMnFe) crystals are biaxial (+), with  $\alpha = 1.608(3)$ ,  $\beta = 1.612(3)$ ,  $\gamma = 1.624(3)$  and  $2V(\text{meas.}) = 59(1)^\circ$ . The empirical formula from electron microprobe analyses and structure refinement is  $(\text{Ca}_{0.70}\text{Mn}_{0.30})\text{Mn}(\text{Fe}_{1.23}^{2+}\text{Mn}_{0.49}\text{Mg}_{0.29}\text{Zn}_{0.06})(\text{Al}_{1.88}\text{Fe}_{0.12}^{3+})(\text{PO}_4)_{3.96}(\text{OH})_2(\text{H}_2\text{O})_8$ . Whiteite-(CaMnFe) is monoclinic,  $P2/a$ ,  $a = 14.925(5)$ ,  $b = 7.0100(14)$ ,  $c = 10.053(2) \text{ \AA}$ ,  $\beta = 111.31(2)^\circ$ ,  $V = 979.9(4) \text{ \AA}^3$  and  $Z = 2$ . The crystal structure was refined using single-crystal data to  $wR_{\text{obs}} = 0.052$  for 1613 reflections with  $I > 3\sigma(I)$ . Site occupancy refinements confirm the ordering of dominant Ca, Mn and  $\text{Fe}^{2+}$  in the  $X$ ,  $M1$  and  $M2$  sites, respectively, of the general jahnsite-group formula  $XM1M2_2M3_2(\text{H}_2\text{O})_8(\text{OH})_2(\text{PO}_4)_4$ .

## 1 Introduction

Whiteite-(CaMnFe) was first identified as a potential new jahnsite-group species during a study of phosphate mineralisation in specimens collected (by EK) from the 60 to 67 m level of the Hagendorf-Süd pegmatite mine (Grey et al., 2010). The mineral was found as inclusions in millimetre-sized waxy nodules of nordgauite,  $\text{MnAl}_2(\text{PO}_4)_2(\text{F},\text{OH})_2 \cdot 5\text{H}_2\text{O}$ , occurring in cavities in etched zwieselite. Strong Al/Fe zoning in those whiteite crystals prevented the complete characterisation required for a new mineral naming proposal.

Recently, a study of Hagendorf-Süd secondary phosphate minerals in the Erich Keck Collection at the Mineralogical State Collection Munich by RH and CR identified a new specimen of whiteite-(CaMnFe) containing compositionally homogeneous crystals of the mineral. Full characterisation of the mineral led to its approval as a new species by the International Mineralogical Association (IMA) Commission on New Minerals, Nomenclature and Classification (CNMNC), IMA2022-072. The approved name is in accordance with the scheme originally proposed by Moore and Ito (1978) for jahnsite-group minerals with general formula  $XM1M2_2M3_2(\text{H}_2\text{O})_8(\text{OH})_2(\text{PO}_4)_4$ . The jahnsite-group nomenclature was recently approved by the IMA CN-

MNC (Kampf et al., 2019). The whiteite root name signifies that the  $M3$  site is occupied by  $Al^{3+}$ , and the suffix indicates that Ca, Mn and Fe are dominant at the  $X$ ,  $M1$  and  $M2$  sites, respectively. The holotype specimen is housed in the collections of the Mineralogical State Collection Munich (SNSB), with the registration number MSM 38031.

## 2 Occurrence, paragenesis and geology

The holotype specimen, Hag107, containing whiteite-(CaMnFe), comes from the Hagendorf-Süd pegmatite, Oberpfalz, Bavaria, Germany (49°39'1" N, 12°27'35" E). The pegmatite at Hagendorf-Süd is a zoned pegmatite body embedded in Variscan biotite gneisses. It can be considered a pegmatitic rest differentiate of the Upper Carboniferous Floßenbürg granite (Fischer, 1965). The pegmatite had the form of a hat, with an oval base of 100 and 200 m in diameter and 150 m from the base to the top (Strunz, 1974). It contained about 1.8 million tonnes of feldspar, 2.7 million tonnes of quartz and about 3000 t of phosphates (Keck, 1983, 1990). The majority were triphylite (about 2000 t) and zwieselite (about 700 t). Derived from these primary phosphates are rockbridgeite (about 200 t) and a multitude of further secondary phosphate minerals.

The phosphate pods were concentrated from a 40 m level down to a 115 m level at the contact of the quartz core with the feldspar masses. Especially in the upper levels many of the primary phosphates were heavily altered due to the influence of vadose waters, with rockbridgeite as the main secondary mineral. The many cavities in the place of the altered primary phosphates (some connected, some enclosed) gave rise to a multitude of secondary phosphates. The different oxygen partial pressures in the different cavities lead to ferrous minerals, minerals with different ratios of combined ferrous and ferric iron, and even minerals with manganese in higher oxidation levels, often to be found in the same sample over few centimetres.

The holotype specimen containing whiteite-(CaMnFe) consists of massive intergrown phosphates, comprising predominantly rockbridgeite intergrown with quartz, mica and feldspar. The secondary phosphates are derived from earlier triphylite, relics of which are intergrown with quartz. Tiny vugs in the rockbridgeite contain spheres of lilac strengite and yellow crystals of laueite, as well as massive intergrown patches of a jahnsite-group mineral. A larger vug (about 1 cm in diameter) in the feldspar-bearing portion of the sample contains masses of tiny tabular pinkish crystals of hureaulite and prismatic crystals of colourless to light brown whiteite-(CaMnFe) (Fig. 1). These minerals formed more or less contemporaneously, as they are sitting on the hureaulite crystals but are also sometimes overgrown by crusts of tiny hureaulites. Strengite, laueite and rockbridgeite are not in direct contact with whiteite-(CaMnFe) or hureaulite. The feldspar along the edge of the vug appears to be corroded and

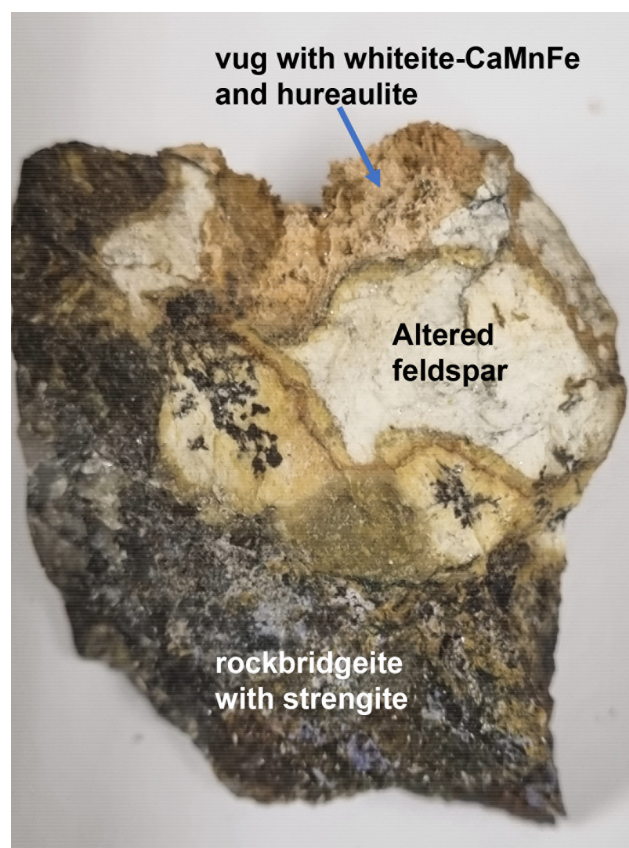


**Figure 1.** Specimen Hag107, showing vug containing whiteite-(CaMnFe) crystals.

is conjectured to be the source of the aluminium in whiteite-(CaMnFe).

Mücke (1981) has published a paragenetic classification of phosphate minerals at Hagendorf-Süd. Jahnsite-(CaMnFe) and associated minerals fit in his paragenesis table IIC, involving rockbridgeite-bearing subparageneses derived from triphylite.

## 3 Physical and optical properties

Whiteite-(CaMnFe) forms sprays and clusters of colourless to pale yellow interlocking rod-like crystals, with diameters of typically 10 to 50  $\mu\text{m}$  and lengths up to  $\sim 500 \mu\text{m}$  (Fig. 2). Scanning electron microscope (SEM) images show that the crystals are composed of sub-parallel growth of laths that are only a few micrometres in width (Fig. 3). The laths are flattened on  $\{001\}$  and elongated along  $[010]$ . A crystal structure analysis showed the presence of twinning by a  $180^\circ$  rotation about  $[100]$ . The measured density, by flotation in mixtures of methylene iodide and toluene, is  $2.80(2) \text{ g cm}^{-3}$ . The calculated density for the empirical formula and single-crystal unit-cell volume is  $2.78 \text{ g cm}^{-3}$ .



**Figure 2.** Whiteite-(CaMnFe) crystals, FOV = 0.58 mm. Photo taken by Christian Rewitzer.

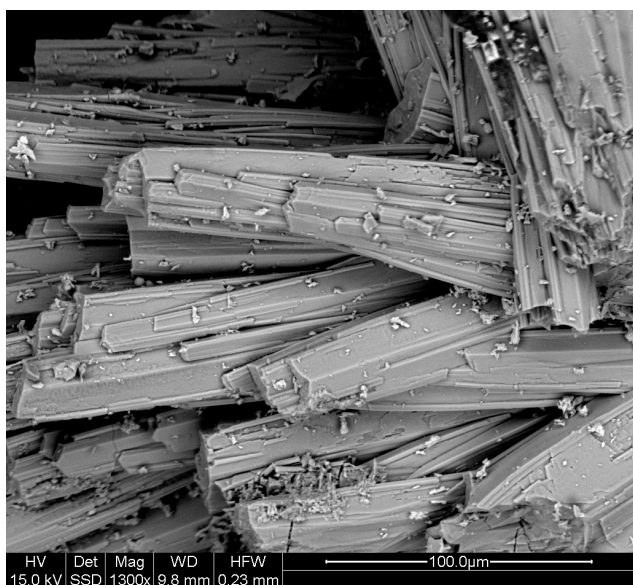


**Figure 3.** BSE image ( $\times 1300$ ) of whiteite-(CaMnFe) crystals.

Optically, whiteite-(CaMnFe) crystals are biaxial (+), with  $\alpha = 1.608(3)$ ,  $\beta = 1.612(3)$  and  $\gamma = 1.624(3)$  (measured in white light). The measured  $2V$  from extinction data analysed with EXCALIBR (Gunter et al., 2004) is  $59(1)^\circ$ , and the calculated  $2V$  is  $60.4^\circ$ . Dispersion and pleochroism were not observed. The partially determined optical orientation is  $Y = b$ . The Gladstone–Dale compatibility index (Mandarino, 1981) is 0.007 (superior) based on the empirical formula and the measured density.

**Table 1.** Analytical data (wt %) for whiteite-(CaMnFe).

Constituent	Mean	Range	SD	Standard
CaO	4.80	3.68–5.58	0.55	Apatite
MnO	15.40	13.43–17.01	0.92	MnSiO <sub>3</sub>
ZnO	0.57	0.14–1.21	0.26	Phosphophyllite
MgO	1.44	1.26–1.62	0.10	Spinel
Al <sub>2</sub> O <sub>3</sub>	11.56	10.95–12.32	0.42	Berlinite
FeO (total)	11.79	9.96–13.74	1.13	Hematite
FeO	10.71			
Fe <sub>2</sub> O <sub>3</sub>	1.20			
P <sub>2</sub> O <sub>5</sub>	34.19	32.96–35.03	0.92	Berlinite
H <sub>2</sub> O*	19.79			
Total	99.66			

\* Based on the ideal formula for whiteite-(CaMnFe).

#### 4 Chemical composition

Crystals of whiteite-(CaMnFe) were mounted in a polished and carbon-coated epoxy block and analysed using wavelength-dispersive spectrometry on a JEOL JXA-8500F Hyperprobe operated at an accelerating voltage of 15 kV and a beam current of 2.2 nA. The beam was defocused to 10  $\mu\text{m}$ . Analytical results (average of analyses on 18 crystals) are given in Table 1. There was insufficient material for direct determination of H<sub>2</sub>O, so it was based upon the crystal structure analysis. The stoichiometric amount of H<sub>2</sub>O (2 H<sub>2</sub>O + 0.5 OH<sup>−</sup> per atom of P) was included in the matrix correction.

The empirical formula based on 26 O<sup>2−</sup> anions, with Fe<sup>2+</sup> at the M2 site and Fe<sup>3+</sup> substituting for Al at the M3 site is (Ca<sub>0.70</sub>Mn<sub>0.30</sub>)Mn<sup>2+</sup>(Fe<sub>1.23</sub><sup>2+</sup>Mn<sub>0.49</sub><sup>2+</sup>Mg<sub>0.29</sub>Zn<sub>0.06</sub>) (Al<sub>1.88</sub>Fe<sub>0.12</sub><sup>3+</sup>)(PO<sub>4</sub>)<sub>3.96</sub>(OH)<sub>2</sub> · 8H<sub>2</sub>O. The simplified formula is (Ca,Mn<sup>2+</sup>)Mn<sup>2+</sup>(Fe<sup>2+</sup>, Mn<sup>2+</sup>, Mg,Zn)<sub>2</sub>(Al, Fe<sup>3+</sup>)<sub>2</sub>(PO<sub>4</sub>)<sub>4</sub>(OH)<sub>2</sub> · 8H<sub>2</sub>O, and the ideal formula is CaMn<sup>2+</sup>Fe<sub>2</sub><sup>2+</sup>Al<sub>2</sub>(PO<sub>4</sub>)<sub>4</sub>(OH)<sub>2</sub> · 8H<sub>2</sub>O, which requires CaO 6.85, FeO 17.55, MnO 8.67, Al<sub>2</sub>O<sub>3</sub> 12.46, P<sub>2</sub>O<sub>5</sub> 34.68, H<sub>2</sub>O 19.79, total 100 wt %.

#### 5 Crystallography

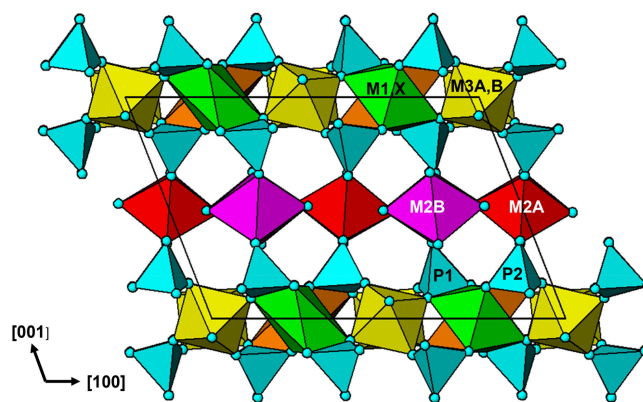
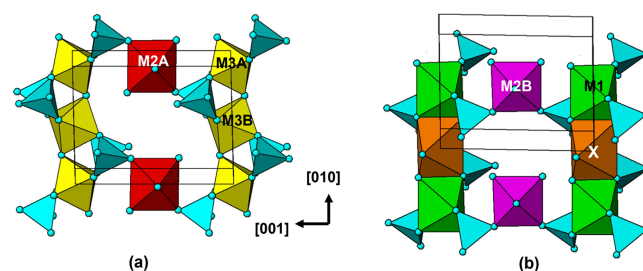
X-ray powder diffraction data were obtained using a Philips X'Pert MPD diffractometer employing Co  $K\alpha$  radiation. Diffraction data in the  $2\theta$  range of 10 to 70° were collected using a step size of 0.033° and a total counting time of 3 h. The total diffraction profile was fitted using the Rietveld programme FullProf (Rodriguez-Carvajal, 1990). Minor hureaultite impurity was included as a second phase. Observed and calculated  $d$  values, intensities and indices are reported in Table 2. Refined monoclinic unit-cell parameters in space group P2/ $a$  are  $a = 14.965(3)$ ,  $b = 6.9990(10)$ ,  $c = 10.084(2)$  Å,  $\beta = 111.31(2)^\circ$  and  $V = 984.0(4)$  Å<sup>3</sup>, with  $Z = 2$ .

**Table 2.** Powder X-ray diffraction data ( $d$  in Å) for whiteite-(CaMnFe).

$I_{\text{obs}}$	$d_{\text{obs}}$	$d_{\text{calc}}$	$hkl$	$I_{\text{obs}}$	$d_{\text{obs}}$	$d_{\text{calc}}$	$hkl$
35	9.397	9.394	0 0 1	4	2.402	2.411	-1 2 3
4	6.972	6.971	2 0 0			2.392	-4 0 4
		6.931	-2 0 1	17	2.330	2.333	-6 1 1
7	5.640	5.649	-1 1 1			2.329	-6 1 2
38	4.932	4.939	2 1 0			2.327	-1 1 4
		4.925	-2 1 1	6	1.997	1.999	6 1 1
7	4.861	4.854	1 1 1			1.996	4 0 3
20	4.707	4.697	0 0 2	18	1.984	1.985	4 2 2
2	4.096	4.090	-1 1 2			1.985	-6 1 4
12	3.962	3.971	2 1 1			1.982	-4 0 5
		3.949	-2 1 2	10	1.976	1.974	-4 2 4
8	3.741	3.741	-4 0 1	20	1.950	1.951	0 2 4
20	3.493	3.485	4 0 0	6	1.920	1.918	2 3 2
18	3.470	3.466	-4 0 2			1.914	-2 3 3
6	3.253	3.249	3 1 1	17	1.871	1.871	-8 0 2
7	3.134	3.131	0 0 3	9	1.750	1.751	0 4 0
4	3.037	3.036	2 1 2	3	1.714	1.716	2 3 3
29	2.923	2.938	4 0 1			1.712	-2 3 4
		2.915	-4 0 3	3	1.640	1.642	-6 3 3
5	2.902	2.902	-3 1 3			1.639	0 4 2
10	2.834	2.832	2 2 1	14	1.565	1.566	0 0 6
100	2.807	2.806	0 2 2			1.563	4 4 0

Single-crystal diffraction data were collected at room temperature using a Rigaku Oxford Diffraction Supernova 4-circle diffractometer equipped with an Atlas CCD detector and using Mo  $K\alpha$  radiation ( $\lambda = 0.71073$  Å). Refined unit-cell parameters and other data collection information are given in Table 3. A structural model was obtained in space group  $P2/n$  using SHELXT (Sheldrick, 2015). The model was transformed to  $P2/a$  to be consistent with other published jahnsite-group minerals and refined using JANA2006 (Petříček et al., 2014). Scattering curves for Ca, Mn, Fe and Al were used for the sites X, M1, M2 and M3, respectively, of the general formula for jahnsite-group minerals,  $XM_1M_2M_3_2(H_2O)_8(OH)_2(PO_4)_4$  (Kampf et al., 2019). Twinning by a  $180^\circ$  rotation about [100] was implemented. Refinement with anisotropic displacement parameters for all non-hydrogen atoms converged at  $wR_{\text{obs}} = 0.050$  for 1640 reflections with  $I > 3\sigma(I)$ . The unambiguous location of H atoms in difference Fourier maps was not achieved, most likely because the data quality was compromised by the crystal being composed of subparallel laths, as shown in Fig. 3. Complete H positions have previously been reported for whiteite-(MnMnMg) (Capitelli et al., 2011) and whiteite-(CaMgMg) (Kampf et al., 2016).

Details of the crystal structure refinement are given in Table 3. The refined coordinates, equivalent isotropic displacement parameters and bond valence sum (BVS) values (Gagné and Hawthorne, 2015) from the single-crystal refinement are reported in Table 4. Selected interatomic distances are reported in Table 5. Although the H atoms were not located,

**Figure 4.** The [010] projection of the whiteite-type structure using ATOMS (Dowty, 2006).**Figure 5.** The [100] projections of (a) strunzite-type and (b) large cation-containing (100) layers in the whiteite-type structure.

the BVSs in Table 4 show clearly that O9 is an OH group and that O10, O11, O12 and O13 are  $H_2O$  groups.

## 6 Discussion

A projection of the structure for jahnsite-group minerals along [010] is shown in Fig. 4 with the cation sites labelled. Assignment of the EMP-analysed cation contents to the different cation sites of the general jahnsite-group formula using the procedure described by Kampf et al. (2019) gives the rounded structural formula  $(Ca_{0.7}Mn_{0.3})Mn(Fe_{1.2}Mn_{0.5}Mg_{0.3})(Al_{1.9}Fe_{0.1})(PO_4)_4(OH)_2(H_2O)_8$ . The BVS values given in Table 4 are generally consistent with this formula, with predominantly divalent cations in the X, M1 and M2 sites and trivalent cations in the M3 sites. The BVS values in Table 4 were calculated for the ideal formula,  $CaMn^{2+}Fe_2^{2+}Al_2(PO_4)_4(OH)_2 \cdot 8H_2O$ , cation assignments. As seen from Table 4, the BVS values for Ca and Mn are slightly higher and lower, respectively, than 2, indicating some minor mixing of  $Mn^{2+}$  at the X site and Ca at the M1 site. The BVS values for the M2 sites, 2.13 and 2.15, suggest some minor  $Fe^{3+}$  in these sites, while the BVS values for the M3 sites, 2.92 and 2.90, are consistent with minor substitution of  $Fe^{3+}$  for Al in these sites.

**Table 3.** Crystal data and structure refinement for whiteite-(CaMnFe).

Formula (simplified)	$\text{CaMn}^{2+}\text{Fe}_2^{2+}\text{Al}_2(\text{PO}_4)_4(\text{OH})_2 \cdot 8\text{H}_2\text{O}$
Formula weight	800.5
Temperature	294 K
Wavelength	0.71073 Å
Space group	$P2/a$
Unit-cell dimensions	$a = 14.925(5)$ Å $b = 7.0100(14)$ Å $c = 10.053(2)$ Å $\beta = 111.31(3)^\circ$
Volume	979.9(4) Å <sup>3</sup>
Z	2
Absorption correction	Gaussian, $\mu = 3.27 \text{ mm}^{-1}$
Crystal size	$0.034 \times 0.052 \times 0.145 \text{ mm}^3$
Theta range for data collection	2.91 to 29.96°
Index ranges	$-19 \leq h \leq 20$ , $-8 \leq k \leq 9$ , $-13 \leq l \leq 10$
Reflections collected	6891
Independent reflections	2354
Reflections with $I_o > 3\sigma(I)$	1613
Refinement method	Full-matrix least-squares on $F$
Data/constraints/parameters	2354/17/149
Final $R$ indices [ $I > 3\sigma(I)$ ]	$R_{\text{obs}} = 0.070$ , $wR_{\text{obs}} = 0.052$
$R$ indices (all data)	$R_{\text{obs}} = 0.106$ , $wR_{\text{obs}} = 0.055$
Largest diff. peak and hole	1.33 and $-1.29 e \text{ Å}^{-3}$

**Table 4.** Atom coordinates, equivalent isotropic displacement parameters (Å<sup>2</sup>) and bond valence sums (BVS in valence units) for whiteite-(CaMnFe).

	$x$	$y$	$z$	$U_{\text{eq}}$	BVS
Ca	-0.75	-0.0214(2)	0	0.0163(7)	2.12
Mn1	-0.25	0.5217(2)	0	0.0180(6)	1.87
Fe2a	-0.5	0	-0.5	0.0160(5)	2.13
Fe2b	-0.75	0.49760(16)	-0.5	0.0165(5)	2.15
Al3a	-0.5	0	0	0.0076(9)	2.92
Al3b	-0.5	0.5	0	0.0112(10)	2.90
P1	-0.67720(11)	0.2565(2)	-0.18657(16)	0.0152(5)	5.05
P2	-0.41893(12)	0.24958(19)	-0.19610(17)	0.0129(5)	5.26
O1	-0.6334(3)	0.4381(6)	-0.0956(5)	0.0220(16)	1.92
O2	-0.7071(5)	0.2915(6)	-0.3440(5)	0.0285(18)	1.77
O3	-0.7689(3)	0.2275(7)	-0.1508(5)	0.0307(18)	1.87
O4	-0.6170(4)	0.0804(7)	-0.1371(6)	0.050(2)	2.00
O5	-0.4575(4)	0.2224(5)	-0.3543(5)	0.0215(15)	1.78
O6	-0.3104(3)	0.2922(7)	-0.1448(5)	0.0321(19)	1.92
O7	-0.4270(4)	0.0693(6)	-0.1173(5)	0.034(2)	1.99
O8	-0.4719(4)	0.4146(6)	-0.1608(5)	0.0280(18)	1.83
O9	-0.5213(3)	0.7501(6)	-0.0821(4)	0.0167(14)	1.01
O10	-0.5448(5)	0.2171(6)	-0.6587(5)	0.0332(13)	0.35
O11	-0.6375(4)	0.0040(6)	-0.4796(7)	0.0274(14)	0.34
O12	-0.8958(4)	0.5120(6)	-0.5100(8)	0.0251(12)	0.34
O13	-0.7219(5)	0.7222(6)	-0.3380(6)	0.0323(13)	0.30

**Table 5.** Polyhedral bond lengths [ $\text{\AA}$ ] for whiteite-(CaMnFe).

Ca-O3 $\times$ 2	2.261(5)	Mn1-O1 $\times$ 2	2.291(5)
Ca-O6 $\times$ 2	2.363(5)	Mn1-O3 $\times$ 2	2.271(5)
Ca-O7 $\times$ 2	2.493(5)	Mn1-O6 $\times$ 2	2.137(5)
Ca-O4 $\times$ 2	2.887(6)	av	2.233
av	2.501		
Fe2a-O5 $\times$ 2	2.075(4)	Fe2b-O2 $\times$ 2	2.056(4)
Fe2a-O10 $\times$ 2	2.129(5)	Fe2b-O12 $\times$ 2	2.144(6)
Fe2a-O11 $\times$ 2	2.136(7)	Fe2b-O13 $\times$ 2	2.193(5)
av	2.113	av	2.131
Al3a-O4 $\times$ 2	1.876(5)	Al3b-O1 $\times$ 2	1.919(4)
Al3a-O7 $\times$ 2	1.936(6)	Al3b-O8 $\times$ 2	1.908(6)
Al3a-O9 $\times$ 2	1.913(4)	Al3b-O9 $\times$ 2	1.915(4)
av	1.908	av	1.919
P1-O1	1.565(4)	P2-O5	1.494(5)
P1-O2	1.500(5)	P2-O6	1.540(5)
P1-O3	1.549(6)	P2-O7	1.519(5)
P1-O4	1.501(5)	P2-O8	1.514(5)
av	1.529	av	1.517

The crystal structure for jahnsite–whiteite minerals is usually described in reference to (001) heteropolyhedral layers. The layers are built from [010] chains of *trans*-corner-connected [ $M3(\text{OH})_2(\text{O}_p)_4$ ] octahedra ( $\text{O}_p = \text{O}$  atom of a  $\text{PO}_4$  group), decorated with  $\text{PO}_4$  tetrahedra and linked along [100] with [010] chains of edge-shared  $M1$ - and  $X$ -centred polyhedra. The heteropolyhedral slabs are interconnected along [001] by the  $\text{PO}_4$  tetrahedra corner-sharing via  $\text{O}_p$  anions to [ $M2(\text{O}_p)_2(\text{H}_2\text{O})_4$ ] octahedra (Fig. 4).

An alternative description in terms of (100) layers gives a different perspective on the structure. As seen in Fig. 4, the structure contains an alternation of two types of (100) layers. These are illustrated in projection normal to the layers in Fig. 5. One layer, Fig. 5a, contains [010] *trans*-corner-connected chains of  $M3$ -centred octahedra that are connected along [001] by *trans*-corner-sharing of  $\text{P}2\text{O}_4$  tetrahedra with  $M2A$ -centred octahedra, while the second layer, Fig. 5b, contains [010] chains of edge-shared  $M1$ - and  $X$ -centred polyhedra that are connected along [001] by *cis*-corner-sharing of  $\text{P}1\text{O}_4$  tetrahedra with  $M2B$ -centred octahedra.

The layer shown in Fig. 5a has the same topology as a (010) layer in strunzite. We have previously reported on the association between corroded Al-bearing jahnsite laths grading into fibrous Al-bearing strunzite at Hagendorf-Süd (Grey et al., 2012). The orientation relationship between the two minerals, with their  $7 \text{\AA}$  axes parallel and the close match between their chemical compositions is consistent with strunzite being derived from jahnsite by selective leaching of the (100)<sub>jahnsite</sub> layers shown in Fig. 5b, containing the more weakly bonded, large divalent  $M1$  and  $X$  cations, followed by linkage of the strunzite-type layers shown in Fig. 5a. This

type of selective leaching, if applied to a whiteite-subgroup mineral, would lead to the formation of a new Al-dominant strunzite species. Such a species has not been reported to date.

The approval of whiteite-(CaMnFe) brings the number of whiteite-subgroup members of the jahnsite group to nine. Information on unit-cell parameters and site assignments for the nine members is summarised in Table 6. Clear relationships exist between the unit-cell parameters and cation assignments in specific sites. The unit-cell  $a$  parameter is inversely related to the size of the cations occupying the  $M1$  and  $X$  sites, as previously discussed by Grey et al. (2020, 2021). This is seen in Table 6 from the progressive increase in the  $a$  parameter with a decrease in the mean  $\langle X\text{-O} \rangle_{\text{oct}}$  bond length. The  $X$  cation in jahnsite-group minerals is usually described as having 8-fold antiprismatic coordination. The  $X\text{-O}$  distances, however, comprise six distances in a relatively narrow range, 2.2 to 2.5  $\text{\AA}$ , with two longer distances, typically 2.8 to 3.1  $\text{\AA}$ ; so the coordination is better described as bi-capped octahedral.

The  $b$  parameter relates to the [010] chains of corner-shared  $M3$ -centred octahedra and edge-shared  $M1$ - and  $X$ -centred octahedra shown in Fig. 5. It is the former that controls the magnitude of the parameter. Whiteite-subgroup minerals with Al in  $M3$  all have  $b$  parameters in a narrow range, 6.89 to 7.05  $\text{\AA}$  (Table 6), while jahnsite-subgroup members with  $\text{Fe}^{3+}$  in  $M3$  all have larger  $b$  values in the range 7.14 to 7.19  $\text{\AA}$  (Grey et al., 2020), with no correlation between  $b$  and the size of the  $M1$  and  $X$  cations.

The  $c$  parameter, as a measure of the separation of the (001) heteropolyhedral layers, would be expected to correlate with the size of the  $M2$ -centred octahedra that connects

Table 6. Crystallochemical data for whiteite-subgroup minerals.

	CaMgMg	CaMnMg*	CaFeMg	CaMnMn	CaMnFe	MnFeMg*	MnMnMg	MnMnFe*	MnMnMn
<i>a</i> (Å)	14.852	14.842	14.870	14.941	14.965	14.99	15.010	15.01	15.023
<i>b</i> (Å)	7.053	6.976	6.978	6.949	6.999	6.96	6.949	6.89	6.949
<i>c</i> (Å)	9.979	10.109	9.927	10.054	10.084	10.14	9.986	10.16	10.013
$\beta$ (°)	110.17	112.59	110.11	111.31	111.31	110.1	111.09	112.8	110.79
<i>V</i> (Å <sup>3</sup> )	981.0	966.3	967.3	984.0	979.9	993.5	971.9	968.6	977.0
<i>X</i>	Ca	0.76 Ca + 0.24 Mn <sup>2+</sup>	0.9 Ca + 0.1 Na	0.65 Ca + 0.1 Na + 0.25 Zn	0.7 Ca + 0.3 Mn <sup>2+</sup>	0.2 Ca + + 0.6 Mn <sup>2+</sup>	0.60 Mn <sup>2+</sup> + 0.40 Ca	0.54 Mn <sup>2+</sup> 0.46 Ca	0.59 Mn <sup>2+</sup> + 0.38 Ca + 0.03 Na
< <i>X-O</i> >**	2.514 2.427	2.513 2.413	2.513 2.413	2.510 2.397	2.501 2.372	2.501 2.372	2.50 2.309		2.506 2.328
<i>M1</i>	0.69 Mg + 0.31 Ca	Mn	0.9 Fe <sup>2+</sup> + 0.17 Mg	Mn <sup>2+</sup>	Mn <sup>2+</sup>	0.9 Fe <sup>2+</sup> + 0.1 Mn <sup>2+</sup>	0.92 Mn <sup>2+</sup> + 0.08 Mg	Mn <sup>2+</sup>	Mn <sup>2+</sup>
< <i>M1-O</i> >	2.183	2.155	2.155	2.230	2.233	2.233	2.220		2.222
<i>M2</i>	Mg	1.78 Mg + 0.17 Fe <sup>2+</sup> + 0.05 Mn <sup>2+</sup>	Mg	1.0 Mn + 0.68 Fe <sup>2+</sup> + 0.32 Mg, Zn	1.2 Fe <sup>2+</sup> + 0.5 Mn <sup>2+</sup> + 0.3 Mg	Mg	Mg	1.15 Fe <sup>2+</sup> + 0.56 Mn <sup>2+</sup> + 0.29 Mg	1.0 Mn <sup>2+</sup> + 0.55 Fe <sup>3+</sup> + 0.22 Fe <sup>2+</sup> + 0.23 Mg, Zn
< <i>M2A-O</i> >	2.076	2.067	2.075	2.111	2.113	2.113	2.075		2.093
< <i>M2B-O</i> >	2.083	2.075	2.075	2.153	2.131	2.131	2.083		2.142
<i>M3</i>	1.9 Al + 0.1 Mg	Al	Al	1.9 Al + 0.1 Fe <sup>3+</sup>	1.9 Al + 0.1 Fe <sup>3+</sup>	Al	1.82 Al + 0.18 Mn <sup>3+</sup>	1.75 Al + 0.25 Fe <sup>3+</sup>	Al
< <i>M3A-O</i> >	1.928	1.914	1.909	1.883	1.908	1.908	1.911		1.905
< <i>M3B-O</i> >	1.920	1.909	1.909	1.898	1.919	1.919	1.913		1.907
Ref	1	2	3	4	5	6	7	8	

(1) Kampf et al. (2016); (2) Grice et al. (1989); (3) Capitelli et al. (2011); (4) Grey et al. (2010); (5) Moore and Ito (1978); (6) Elliott and Willis (1989); (7) Marzoni et al. (1989); (8) Grey et al., 2021. \* No crystal structure refinements reported for these minerals.  
\*\* First line of numbers is the average of eight X–O bonds; second line is the average of the six shortest X–O bonds.

the layers. Although there is a correlation between  $c$  (or the layer separation  $c\sin\beta$ ) and the mean  $\langle M2-O \rangle$  distances, it is relatively weak. It is likely that the rotations of the  $M3$ -centred octahedra, in response to different-sized  $M1$  and  $X$  cations, also contribute to the  $c$  parameter dimension.

*Data availability.* Crystallographic data for tomsquarryite are available in the Supplement.

*Supplement.* The supplement related to this article is available online at: <https://doi.org/10.5194/ejm-35-95-2023-supplement>.

*Author contributions.* IEG oversaw the research and wrote the paper; RH, CR and EK supplied specimens. CR obtained optical images of the specimen. RH and CR obtained preliminary SEM data that identified the mineral as a new species. WGM assisted in the diffraction data analysis, CMM conducted the microprobe analyses, ARK measured the optical properties, RWG collected the single-crystal diffraction data and AMG obtained the SEM BSE image.

*Competing interests.* The contact author has declared that none of the authors has any competing interests.

*Disclaimer.* Publisher's note: Copernicus Publications remains neutral with regard to jurisdictional claims in published maps and institutional affiliations.

*Acknowledgements.* We thank Cameron Davidson for the preparation of samples for EMP analyses. We acknowledge the Diffraction Laboratory at CSIRO Mineral Resources, Clayton, for the use of their Philips X'Pert MPD diffractometer.

*Review statement.* This paper was edited by Cristian Biagioni and reviewed by Radek Škoda, Yves Moëlo and one anonymous referee.

## References

Capitelli, F., Chita, G., Cavallo, A., Bellatreccia, F., and Della Ventura, G.: Crystal structure of whiteite-(CaFeMg) from Crosscut Creek, Canada, *Z. Kristallogr.*, 226, 731–738, 2011.

Dowty, E.: ATOMS, Shape Software, Kingsport, Tennessee, USA, 2006.

Elliott, P. and Willis, A. C.: Whiteite-(MnMnMg), a new jahnsite-group mineral from Iron Monarch, South Australia: Description and crystal structure, *Can. Mineral.*, 57, 215–223, 2019.

Fischer, G.: Über die modale Zusammensetzung der Eruptiva im ostbayerischen Kristallin, *Geologica Bavarica*, 55, 7–23, 1965.

Gagné, O. C. and Hawthorne, F. C.: Comprehensive derivation of bond-valence parameters for ion pairs involving oxygen, *Acta Crystallogr. B*, 71, 562–578, 2015.

Grey, I. E., Mumme, W. G., Neville, S. M., Wilson, N. C., and Birch, W. D.: Jahnsite-whiteite solid solutions and associated minerals in the phosphate pegmatite at Hagendorf-Süd, Bavaria, Germany, *Mineral. Mag.*, 74, 969–978, 2010.

Grey, I. E., MacRae, C. M., Keck, E., and Birch, W. D.: Aluminium-bearing strunzite derived from jahnsite at the Hagendorf-Süd pegmatite, Germany, *Mineral. Mag.*, 76, 1165–1174, 2012.

Grey, I. E., Keck, E., Kampf, A. R., MacRae, C. M., Cashion, J. D., and Glenn, A. M.: Jahnsite-(CaMnZn) from the Hagendorf Süd pegmatite, Oberpfalz, Bavaria, and structural flexibility of jahnsite-group minerals, *Mineral. Mag.*, 84, 547–553, 2020.

Grey, I. E., Smith, J. B., Kampf, A. R., Mumme, W. G., MacRae, C. M., Riboldi-Tunncliffe, A., Boer, S., Glenn, A. M., and Gable, R. W.: Whiteite-(MnMnMn), a new jahnsite-group mineral species from the Foote mine, North Carolina, USA, and chemical pressure effects in jahnsite-group minerals, *Mineral. Mag.*, 85, 862–867, 2021.

Grice, J. D., Dunn, P. J., and Ramik, R. A.: Whiteite-(CaMnMg), a new mineral species from the Tip Top pegmatite, Custer, South Dakota, *Can. Mineral.*, 27, 699–702, 1989.

Gunter, M. E., Bandli, B. R., Bloss, F. D., Evans, S. H., Su, S. C., and Weaver, R.: Results from a McCrone spindle stage short course, a new version of EXCALIBR, and how to build a spindle stage, *The Microscope*, 52, 23–39, 2004.

Kampf, A. R., Adams, P. M., and Nash, B. P.: Whiteite-(CaMgMg),  $\text{CaMg}_3\text{Al}_2(\text{PO}_4)_4(\text{OH})_2 \cdot 8\text{H}_2\text{O}$ , a new jahnsite-group mineral from the Northern Belle mine, Candelaria, Nevada, USA, *Can. Mineral.*, 54, 1513–1523, 2016.

Kampf, A. R., Alves, P., Kasatkin, A., and Škoda, R.: Jahnsite-(MnMnZn), a new jahnsite-group mineral, and formal approval of the jahnsite group, *Eur. J. Mineral.*, 31, 167–172, 2019.

Keck, E.: Phosphatminerale und deren Auftreten in verschiedenen Teufen im Pegmatit von Hagendorf-Süd, *Der Aufschluss*, 34, 307–316, 1983.

Keck, E.: Hagendorf-Süd, Ein kurzer historischer Überblick, *Der Aufschluss*, 41, 53–66, 1990.

Mandarino, J. A.: The Gladstone-Dale relationship: Part IV. The compatibility concept and its application, *Can. Mineral.*, 19, 441–450, 1981.

Marzoni Fecia Di Cossato, Y., Orlandi, P., and Vezzalini, G.: Rittmanite, a new mineral species of the whiteite group from the Mangualde granitic pegmatite, Portugal, *Can. Mineral.*, 27, 447–449, 1989.

Moore, P. B. and Ito, J.: I. Whiteite, a new species, and a proposed nomenclature for the jahnsite-whiteite complex series, II. New data on xanthoxenite, III. Salmonsites discredited, *Mineral. Mag.*, 42, 309–323, 1978.

Mücke, A.: The paragenesis of the phosphate minerals of the Hagendorf pegmatite – a general view, *Chemie der Erde*, 40, 217–234, 1981.

Petříček, V., Dušek, M., and Palatinus, L.: Crystallographic Computing System JANA2006: General features, *Z. Kristallogr.*, 229, 345–352, 2014.

Rodriguez-Carvajal, J.: FULLPROF: A Program for Rietveld refinement and Pattern Matching Analysis: Satellite meeting on powder diffraction of the Fifteenth General Assembly and International Congress of Crystallography, Toulouse, France, 16–19 July, 1990.

Sheldrick, G. M.: Crystal-structure refinement with SHELX, *Acta Crystallogr. C*, 71, 3–8, 2015.

Strunz, H.: Excursion A1: Granites and pegmatites in Eastern Bavaria, Excursion guidebook, edited by: Troll, G., *Fortschritte der Mineralogie, Beiheft 1*, 51, 1–32, 1974.